HIGH TEMPERATURE MECHANICAL BEHAVIOUR OF CAST IN-SITU TiAl-BASED MATRIX COMPOSITE REINFORCED WITH Ti_2AlC PARTICLES

Juraj LAPIN, Kateryna KAMYSHNYKOVA

Institute of Materials and Machine Mechanics, Slovak Academy of Sciences, Bratislava, Slovak Republic, EU, juraj.lapin@savba.sk, kateryna.kamyshnykova@savba.sk

https://doi.org/10.37904/metal.2019.748

Abstract

Samples of in-situ TiAl-based matrix composite reinforced with Ti_2AlC particles were prepared by vacuum induction melting of a charge with a nominal composition Ti-47Al-5Nb-1C-0.2B (at%) in graphite crucibles and centrifugal casting into a graphite mould. The as-cast samples were subjected to hot isostatic pressing (HIP) and multi-step heat treatments. High temperature compression tests at 1000 °C were carried out on the heat-treated in-situ composite with an optimised microstructure. During compressive deformation, the work hardening is the predominant mechanism at small strains due to an increment of dislocation density in the in-situ composite. At higher strains, dynamic recovery and recrystallization act as main softening mechanisms and exceed the work hardening, which leads to a decrease of the compressive flow stress with increasing strain. The creep deformation curves exhibit a primary creep stage, which is followed by a tertiary creep stage at temperatures ranging from 800 to 900 °C and applied stresses ranging from 150 to 250 MPa. The high temperature creep resistance of the studied in-situ composite is superior compared with that of some TiAl-based alloys with fully lamellar, nearly lamellar, convoluted and pseudo-duplex microstructures at a temperature of 800 °C and applied stress of 200 MPa.

Keywords: TiAl, composites, mechanical behaviour, creep, microstructure

1. INTRODUCTION

Low strength at high temperatures (above 800 °C) limit wide-scale applications of TiAl-based alloys in aircraft and automotive industry [1]. In-situ TiAl-based matrix composites reinforced with carbide particles can improve the deficiency of these lightweight alloys at high temperatures because of a good combination of properties of the intermetallic matrix and the reinforcement [2-4]. Among several types of carbides such as TiC, H-Ti_2AlC, P-Ti_3AlC and N-Ti_3AlC_2 forming in carbon-containing TiAl-based alloys [5], the Ti_2AlC phase possesses high fracture resistance, excellent damage tolerance, good thermal and electrical conductivity, easy machinability, good thermal shock and oxidation resistance, high elastic modulus and thermomechanical stability [6-8]. Coarse primary Ti_2AlC particles formed in a liquid state have shown a significant role in toughening and reinforcing of TiAl-based matrix composites [2,9-11]. The additional strengthening of the in-situ composites can be achieved by fine secondary P-Ti_3AlC and H-Ti_2AlC precipitates similarly to that reported for several low carbon TiAl-based alloys [12-14]. The in-situ composites with lamellar $\alpha_2(Ti_3Al)$ + γ(TiAl) matrix reinforced with the low volume fraction of primary Ti_2AlC particles and fine secondary carbide precipitates show superior high temperature mechanical properties compared to those of the in-situ composites with near γ(TiAl) or duplex type of TiAl-based matrix.

Among various techniques applied for processing of in-situ TiAl-based matrix composites, melting and casting are of large interest for the production of complex-shaped components such as turbocharger wheels, turbine blades or exhaust valves in a cost-effective way [15-18]. Centrifugal casting leads to better surface quality, no misruns in thin sections and fewer cracks compared to those of gravity cast components [3,19]. The centrifugal casting can be combined with different types of melting, but vacuum induction melting is the most frequently used technique due to its flexibility. Microstructure formation and distribution of carbide particles in cast in-situ composites is a complex process strongly affected by solidification and solid-state phase transformations [14].

In spite of the previous studies on in-situ TiAl matrix composites, only limited information is available about their high temperature mechanical behaviour. Hence, to explore the full potential of the carbide reinforcements and develop centrifugally cast in-situ composites with optimised chemical composition and microstructure, it is of large importance to evaluate microstructural aspects affecting their high temperature deformation behaviour.

The aim of this paper is to study high temperature mechanical behaviour of in-situ TiAl-based matrix composite reinforced with carbide particles prepared by vacuum induction melting of Ti-46.4Al-5.1Nb-1C-0.2B (at%) alloy in graphite crucibles and centrifugal casting into a graphite mould. In this alloy, niobium is added to improve oxidation resistance and strength properties at both room and high temperatures. Boron refines grain microstructure and carbon improves creep resistance through the formation of coarse primary and fine secondary carbide particles.

2. EXPERIMENTAL PROCEDURES

Samples of in-situ composite with a nominal composition Ti-46.4Al-5Nb-1C-0.2B (at%) were prepared by vacuum induction melting in graphite crucibles which was followed by a centrifugal casting into a cold graphite mould. The as-cast samples with a diameter of 15 mm and length of 150 mm were subjected to hot isostatic pressing (HIP) at a temperature of 1360 °C, applied pressure of 200 MPa for 4 h to remove casting porosity. The coarse-grained structure of HIP-ed samples was refined by heat treatments consisting of several steps described in detail elsewhere [3,20].

Compression tests were carried out on cylindrical specimens with a diameter of 10 mm and length of 15 mm at a temperature of 1000 °C and initial strain rates ranging from $1x10^{-4}$ to $1x10^{-1}$ s^{-1} using a thermo-mechanical tester Gleeble 3800. The test temperature was measured by a thermocouple spot-welded to the specimen surface. The compression true stress-true strain curves were calculated from the measured engineering compression stress-strain data using the procedure described elsewhere [21].

Cylindrical creep specimens with a gauge diameter of 6 mm and gauge length of 30 mm were lathe machined from the heat-treated samples. Constant load tensile creep tests were carried out at temperatures ranging from 800 to 900 °C under initial stresses ranging from 150 to 250 MPa in air. Elongation was measured using a high temperature extensometer attached to the ledges of the creep specimen. The treatment of creep data was carried out using the procedure described elsewhere [22].

Microstructure evaluation was performed by scanning electron microscopy (SEM), SEM in back-scattered electron (BSE) mode, X-ray diffraction (XRD) analysis and energy-dispersive X-ray spectroscopy (EDS). The average content of carbon was measured by LECO CS844 elemental analyser based on the combustion method. Volume fraction and size of coexisting phases were measured on digitalised SEM and BSE micrographs using a computerised image analyser.

3. RESULTS AND DISCUSSION

3.1. Microstructure characterization

Figure 1 shows the typical microstructure of the centrifugally cast samples. The as-cast microstructure of the samples is chemically inhomogeneous and consists of equiaxed grains with a mean grain size of (53.1 ± 1.2) μm. The XRD analysis has shown that the as-cast composite contains four phases: γ, α_2, Ti_2AlC and TiB [3]. The microstructure within the grains is nearly lamellar and contains well-aligned α_2 and γ plates. The plate-like Ti_2AlC particles are distributed preferentially within the dendrites and ribbon-like TiB particles are formed in the interdendritic region containing the γ phase. The volume fraction and mean length of the Ti_2AlC particles is measured to be (2.3 ± 0.2) vol% and (15.7 ± 0.2) μm, respectively. The inhomogeneous microstructure and casting porosity deteriorates mechanical properties of the as-cast components and

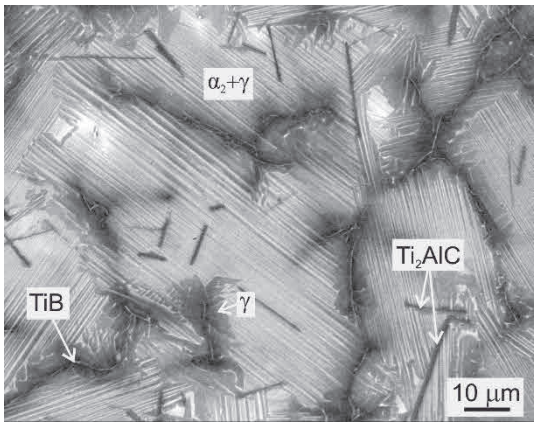

Figure 1 BSE micrograph showing the typical microstructure of centrifugally cast in-situ composite

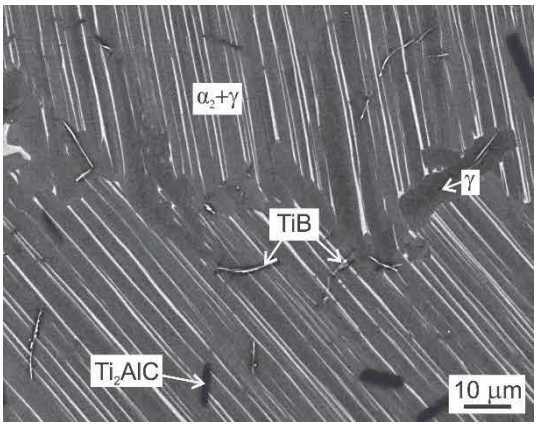

Figure 2 BSE micrographs showing the typical microstructure of compression and creep specimens

increases cracking tendency during the cooling process of the castings [19]. Therefore, the as-cast samples were subjected to HIP to remove the casting porosity and consecutive heat treatments for microstructure optimisation [1,3,20]. **Figure 2** shows the typical microstructure of the compression and creep specimens prepared from the in-situ composite subjected to optimised heat treatments. The fully lamellar coarse-grained microstructure with a mean grain size of (389 ± 15) μm is composed of well-aligned α_2 and γ lamellae, plate-like Ti_2AlC particles and ribbon-like TiB particles. The serrated grain boundaries contain predominantly the γ phase. The creep resistance of TiAl-based alloys is independent of the grain size as far as the grains are larger than about 70-100 μm in fully lamellar alloys [1,3]. However, the coarse-grained microstructure deteriorates room-temperature ductility.

3.2. High-temperature compressive behaviour

Figure 3 shows the typical true stress-true strain compressive curves of the studied in-situ composite at a temperature of 1000 °C. The true stress first increases sharply with increasing true strain. After reaching a peak flow stress, true stress decreases with increasing true strain. **Figure 4** shows the dependence of peak flow stress (PFS) on the applied strain rate at 1000 °C. The measured values of peak flow stress (σ_{PFS}) can be fitted to a power law equation as a function of the applied strain rate $\dot{\varepsilon}$ in the form

$$\sigma_{PFS} = K\dot{\varepsilon}^{m} \quad (1)$$

where *K* is the material constant and *m* is the strain rate exponent. Linear regression analysis leads to a strain rate exponent of *m* = 0.13 at a test temperature of 1000 °C. The true strain to PFS depends on the applied strain rate and increases from 2.8 % to 24.8 % with increasing strain rate from 10^{-4} s^{-1} to 10^{-1} s^{-1}, as shown in **Figure 4**.

For the studied in-situ composite, the work hardening is the predominant mechanism at small strains due to an increment of dislocation density and deformation twins in the intermetallic matrix [23]. At higher strains, the work softening of the in-situ composites results from dynamic recovery and dynamic recrystallization of the lamellar α_2 + γ matrix [23]. The high dislocation density at the matrix/carbide particle interfaces and along the grain boundaries provides the driving force for the nucleation and growth of fine recrystallized γ grains. The shape of the flow curves indicates a good balance between the work hardening and softening mechanisms operating at the temperature as high as 1000 °C, as shown in **Figure 3**. The high peak flow stress and gradual decrease of the flow stress with the inversing true strain indicates a promising high-temperature strength, which is of large interest for future structural applications demanding improved creep resistance.

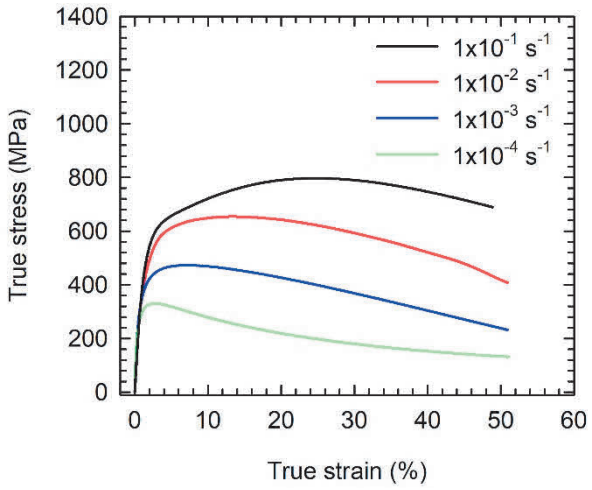

Figure 3 True stress-true strain compressive curves at 1000 °C

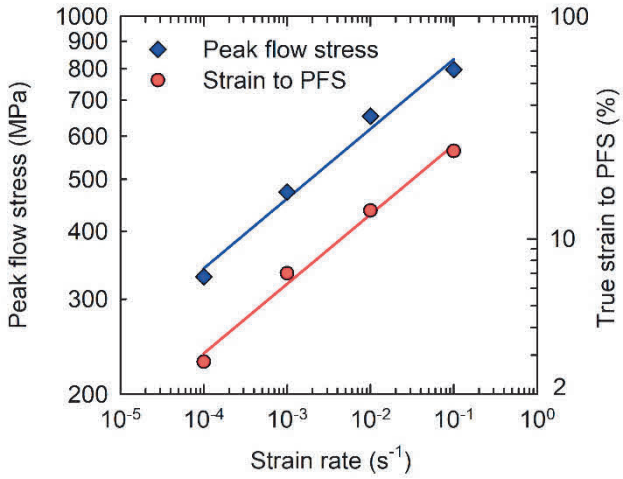

Figure 4 Dependence of peak flow stress (PFS) and true strain to PFS on strain rate at 1000 °C

3.3. Creep behaviour

The creep deformation curves of the studied in-situ composite exhibit short primary creep stage that is directly followed by the tertiary creep, as shown in **Figure 5**. During the primary creep stage, creep rate decreases with increasing strain. After reaching a minimum value, the creep rate increases with increasing strain. **Figure 6** shows the dependence of the measured minimum creep rate on the applied stress at a temperature of 850 °C. The measured minimum creep rates and applied stresses can be fitted to a power law equation described elsewhere [22]. Using linear regression analysis of the creep data, the stress exponent *n* of the power law equation is determined to be 5.1. The stress exponents of about 5 indicate that the kinetics of the creep deformation is controlled by diffusion assisted climb of dislocations.

Figure 7 shows creep deformation curve of the studied in-situ composite (1) compared to those of other TiAl-based alloys tested at a temperature of 800 °C and applied load of 200 MPa. The studied in-situ composite shows improved creep resistance compared to that of Ti-45Al-2W-0.6Si-0.7B (2), Ti-46Al-8Ta (3), Ti-45.5Al-8Nb (4), Ti-46Al-2W-0.5Si (5) and Ti-43.3Al-4Nb-1Mo-0.1B-0.3C-0.3Si (6) (in at%) alloys with fully

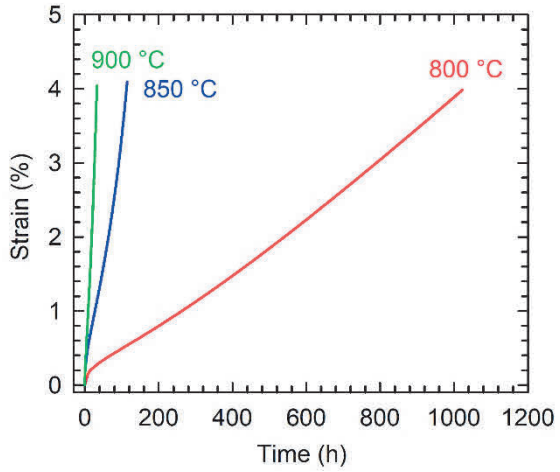

Figure 5 Creep deformation curves at an applied load of 200 MPa

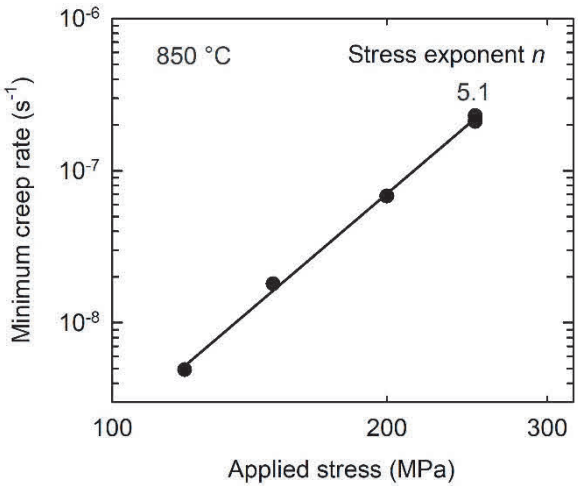

Figure 6 Dependence of minimum creep rate on applied stress at a temperature of 850 °C

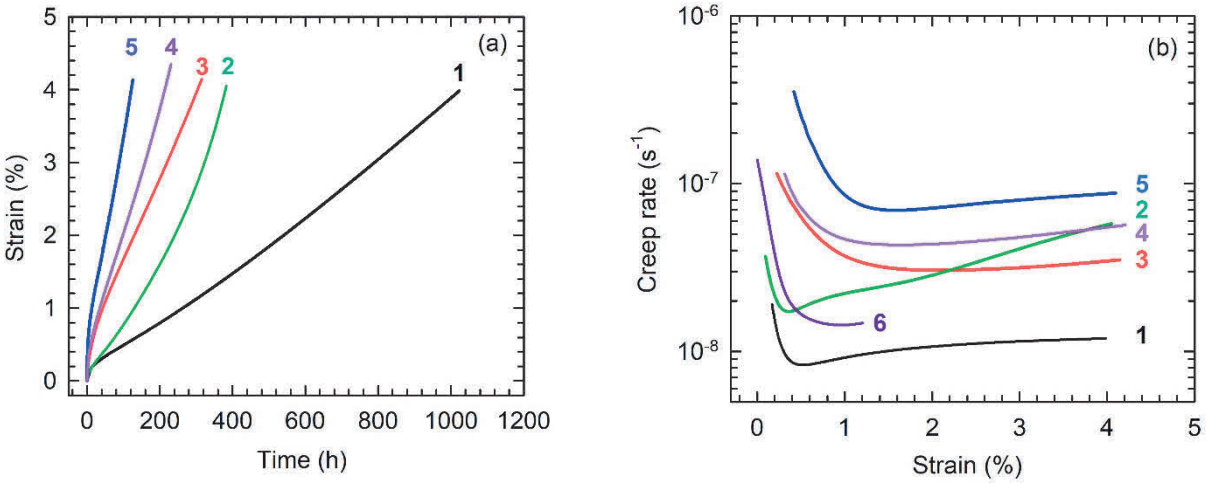

Figure 7 Creep deformation curves at a temperature of 800 °C and applied load of 200 MPa: (a) dependence of strain on time; (b) dependence of creep rate on the strain

lamellar, nearly lamellar, convoluted and pseudo-duplex microstructures, as shown in **Figures 7a** and **7b** [3,24]. The improvement in the creep strength of the studied in-situ composite can be attributed to the stabilisation of fully lamellar $\alpha_2 + \gamma$ microstructure and its reinforcement with the plate-like primary Ti_2AlC particles as well as with fine secondary carbide precipitates formed during the heat treatments and creep exposure. A significant improvement in the creep resistance of carbon-containing TiAl-based alloys has been attributed to dislocation pinning by fine carbides and refinement of the lamellar microstructure [24,25].

4. CONCLUSION

The high temperature mechanical behaviour of cast in-situ TiAl-based matrix composite reinforced with Ti_2AlC particles with a nominal composition Ti-47Al-5Nb-1C-0.2B (at.%) is studied. During high temperature compressive deformation, the peak flow stress and strain to peak flow stress increase with increasing applied strain rate. The creep deformation curves exhibit a short primary creep stage that is directly followed by the tertiary creep. During the primary creep stage, the creep rate decreases with increasing strain. After reaching a minimum value, the creep rate increases with increasing strain. The high temperature creep resistance of the studied in-situ is improved compared to that of some TiAl-based alloys with fully lamellar, nearly lamellar, convoluted and pseudo-duplex microstructures at a temperature of 800 °C and applied load of 200 MPa.

ACKNOWLEDGEMENTS

This work was financially supported by the Slovak Research and Development Agency under the contract APVV-15-0660.

REFERENCES

[1] KIM, Y.W. and KIM, S.L. Advances in gammalloy materials-processes-application technology: Successes, dilemmas, and future. *JOM*. 2018. vol. 70, pp. 553-560. DOI: 10.1007/s11837-018-2747-x.

[2] ŠTAMBORSKÁ, M., LAPIN, J. and BAJANA, O. Effect of carbon on the room temperature compressive behaviour of Ti-44.5Al-8Nb-0.8Mo-xC alloys prepared by vacuum induction melting. *Kovove Mater*. 2018. vol. 56, pp. 349-356. DOI: 10.4149/km_2018_6_349.

[3] LAPIN, J. and KAMYSHNYKOVA, K. Processing, microstructure and mechanical properties of in-situ Ti_3Al+TiAl matrix composite reinforced with Ti_2AlC particles prepared by centrifugal casting. *Intermetallics*. 2018. vol. 98, pp. 34-44. DOI: 10.1016/j.intermet.2018.04.012.

[4] KLIMOVÁ, A. and LAPIN, J. Effects of C and N additions on primary MAX phase particles in intermetallic Ti-Al-Nb-Mo matrix in-situ composites prepared by vacuum induction melting. *Kovove Mater.* 2019. vol. 57, pp. 151-157. DOI: 10.4149/km_2019_3_151.

[5] WITUSIEWICZ, V.T., HALLSTEDT, B., BONDAR, A.A., HECHT, U., SLEPTSOV, S.V. and VELIKANOVA, T.Y. Thermodynamic description of the Al-C-Ti system. *J. Alloys Compd*. 2015. vol. 623, pp. 480-496. DOI: 10.1016/j.jallcom.2014.10.119.

[6] SCABAROZI, T., GANGULY, A., HETTINGER, J.D., LOFLAND, S.E., AMINI, S., FINKEL, P., EL-RAGHY, T. and BARSOUM, M.W. Electronic and thermal properties of $Ti_3Al(C_{0.5},N_{0.5})_2$, $Ti_2Al(C_{0.5},N_{0.5})$ and Ti_2AlN. *J. Appl. Phys*. 2008. vol. 104, pp. 1-7. DOI: 10.1063/1.2979326.

[7] BARSOUM, M.W., ALI, M. and EL-RAGHY, T. Processing and characterization of Ti_2AlC, Ti_2AlN, and $Ti_2AlC_{0.5}N_{0.5}$. *Metall. Mater. Trans. A*. 2000. vol. 31, pp. 1857-1865. DOI: 10.1007/s11661-006-0243-3.

[8] ZHOU, A.G. and BARSOUM, M.W. Kinking nonlinear elastic deformation of Ti_3AlC_2, Ti_2AlC, $Ti_3Al(C_{0.5},N_{0.5})_2$ and $Ti_2Al(C_{0.5},N_{0.5})$. *J. Alloys Compd*. 2010. vol. 498, pp. 62-70. DOI: 10.1016/j.jallcom.2010.03.099.

[9] FANG, H., CHEN, R., GONG, X., SU, Y., DING, H., GUO, J. and FU, H. Effects of Nb on microstructure and mechanical properties of Ti42Al2.6C alloys. *Adv. Eng. Mater*. 2018. vol. 20, pp 1-9. DOI: 10.1002/adem.201701112.

[10] CHEN, R., TAN, Y., FANG, H., LUO, L., DING, H., SU, Y., GUO, J. and FU, H. Macro/microstructure evolution and mechanical properties of Ti33.3Al alloys by adding WC particles. *Mater. Sci. Eng. A*. 2018. vol. 725, pp. 171-180. DOI: 10.1016/j.msea.2018.04.025.

[11] CHEN, R., FANG, H., CHEN, X., SU, Y., DING, H., GUO, J. and FU, H. Formation of TiC/Ti_2AlC and $\alpha_2+\gamma$ in in-situ TiAl composites with different solidification paths. *Intermetallics*. 2017. vol. 81, pp. 9-15. DOI: 10.1016/j.intermet.2017.02.025.

[12] ČEGAN, T. and SZURMAN, I. Thermal stability and precipitation strengthening of fully lamellar Ti-45Al-5Nb-0.2B-0.75C alloy. *Kovove Mater.* 2018. vol. 55, pp. 421-430. DOI: 10.4149/km_2017_6_421..

[13] GABRISCH, H., STARK, A., SCHIMANSKY, F.P., WANG, L., SCHELL, N., LORENZ, U. and PYCZAK, F. Investigation of carbides in Ti-45Al-5Nb-xC alloys ($0 \leq x \leq 1$) by transmission electron microscopy and high energy-XRD. *Intermetallics*. 2013. vol. 33, pp. 44-53. DOI: 10.1016/j.intermet.2012.09.023.

[14] WANG, L., OEHRING, M., LORENZ, U., STARK, A. and PYCZAK, F. New insights into perovskite-Ti_3AlC precipitate splitting in a Ti-45Al-5Nb-0.75C alloy by transmission electron microscopy. *Intermetallics*. 2018. vol. 100, pp. 70-76. DOI: 10.1016/j.intermet.2018.06.006.

[15] BÜNCK, M., STOYANOV, T., SCHIEVENBUSCH, J., MICHELS, H. and GUßFELD, A. Titanium aluminide casting technology development. *JOM*. 2017. vol. 69, pp. 2565-2570. DOI: 10.1007/s11837-017-2534-0.

[16] AGUILAR, J., SCHIEVENBUSCH, A. and KÄTTLITZ, O. Investment casting technology for production of TiAl low pressure turbine blades - Process engineering and parameter analysis. *Intermetallics*. 2011. vol. 19, pp. 757-761. DOI: 10.1016/j.intermet.2010.11.014.

[17] SHOUREN, W., PEIQUAN, G. and LIYING, Y. Centrifugal precision cast TiAl turbocharger wheel using ceramic mold. *J. Mater. Process. Technol*. 2008. vol. 204, pp. 492-497. DOI: 10.1016/j.jmatprotec.2008.01.062.

[18] TETSUI, T., KOBAYASHI, T., UENO, T. and HARADA, H. Consideration of the influence of contamination from oxide crucibles on TiAl cast material, and the possibility of achieving low-purity TiAl precision cast turbine wheels. *Intermetallics*. 2012. vol. 31, pp. 274-281. DOI: 10.1016/j.intermet.2012.07.019.

[19] HARDING, R.A. Recent developments in the induction skull melting and investment casting of titanium aluminides. *Kovove Mater*. 2004. vol. 42, pp. 225-241.

[20] KAMYSHNYKOVA, K. and LAPIN, J. Grain refinement of cast peritectic TiAl-based alloy by solid-state phase transformations. *Kovove Mater*. 2018. vol. 56, pp. 277-287. DOI: 10.4149/km_2018_5_277.

[21] ŠTAMBORSKÁ, M. and LAPIN, J. Effect of anisotropic microstructure on high-temperature compression deformation of CoCrFeNi based complex concentrated alloy. *Kovove Mater*. 2017. vol. 55, pp. 369-378. DOI: 10.4149/km 2017 6 369.

[22] SKLENIČKA, V., KUCHAROVÁ, K., KRÁL, P., KVAPILOVÁ, M.and DVORÁK, J. Applicability of empirical formulas and fractography for assessment of creep life and creep fracture modes of tempered martensitic 9%Cr steel. *Kovove Mater*. 2017. vol. 55, pp. 69-80. DOI: 10.4149/km-2017-2-69.

[23] ZENG, S., ZHAO, A., JIANG, H. and REN, Y. Flow behavior and processing maps of Ti-44.5Al-3.8Nb-1.0Mo-0.3Si-0.1B alloy. *J. Alloys Compd*. 2017. vol. 698, pp. 786-793. DOI: 10.1016/j.jallcom.2016.12.214.

[24] KLEIN, T., USATEGUI, L., RASHKOVA, B., NÓ, M.L., SAN JUAN, J., CLEMENS, H. and MAYER, S. Mechanical behavior and related microstructural aspects of a nano-lamellar TiAl alloy at elevated temperatures. *Acta Mater*. 2017. vol. 128, pp. 440-450. DOI: 10.1016/j.actamat.2017.02.050.

[25] SCHWAIGHOFER, E., RASHKOVA, B., CLEMENS, H., STARK, A. and MAYER, S. Effect of carbon addition on solidification behavior, phase evolution and creep properties of an intermetallic β-stabilized γ-TiAl based alloy. *Intermetallics*. 2014. vol. 46, pp. 173-184. DOI: 10.1016/j.intermet.2013.11.011.